



HAL
open science

Development of a thermosensitive statin loaded chitosan-based hydrogel promoting bone healing

Catherine Petit, Fareeha Batool, Céline Stutz, Nicolas Anton, Andrey Klymchenko, Thierry Vandamme, Nadia Benkirane-Jessel, Olivier Huck

► To cite this version:

Catherine Petit, Fareeha Batool, Céline Stutz, Nicolas Anton, Andrey Klymchenko, et al.. Development of a thermosensitive statin loaded chitosan-based hydrogel promoting bone healing. *International Journal of Pharmaceutics*, 2020, 586, pp.119534. 10.1016/j.ijpharm.2020.119534 . hal-03045178

HAL Id: hal-03045178

<https://hal.science/hal-03045178>

Submitted on 22 Aug 2022

HAL is a multi-disciplinary open access archive for the deposit and dissemination of scientific research documents, whether they are published or not. The documents may come from teaching and research institutions in France or abroad, or from public or private research centers.

L'archive ouverte pluridisciplinaire **HAL**, est destinée au dépôt et à la diffusion de documents scientifiques de niveau recherche, publiés ou non, émanant des établissements d'enseignement et de recherche français ou étrangers, des laboratoires publics ou privés.



Distributed under a Creative Commons Attribution - NonCommercial 4.0 International License

Development of a thermosensitive statin loaded chitosan-based hydrogel promoting bone healing

Catherine Petit ^{1,2,3}, Fareeha Batool ^{1,2}, Céline Stutz ¹, Nicolas Anton ⁴, Andrey Klymchenko ⁵, Thierry Vandamme ⁴, Nadia Benkirane-Jessel ¹, Olivier Huck ^{1,2,3}

¹ INSERM, UMR 1260 ‘Osteoarticular and Dental Regenerative Nanomedicine’, Faculté de Médecine, Fédération de Médecine Translationnelle de Strasbourg (FMTS), Strasbourg, France

² Faculté de Chirurgie Dentaire, Université de Strasbourg, Strasbourg, France

³ Pôle de Médecine et de Chirurgie Bucco-Dentaires, Hôpitaux Universitaires de Strasbourg, Strasbourg, France

⁴ Université de Strasbourg, CNRS, CAMB UMR 7199, Strasbourg, France

⁵ Université de Strasbourg, CNRS, LBP UMR 7021, F-67000 Strasbourg, France

Figure: 9

Tables: 2

Words:

Corresponding author:

Prof. Olivier Huck, Dental faculty, 8 rue Sainte-Elisabeth, 67000 Strasbourg, France;

@: o.huck@unistra.fr; Phone: +33(0)388116947

Abstract

Statins have been proposed as potential adjuvant to periodontal treatment due to their pleiotropic properties. A new thermosensitive chitosan hydrogel loaded with statins (atorvastatin and lovastatin) nanoemulsions was synthesized to allow a spatially controlled local administration of active compounds at lesion site. Spontaneous nano-emulsification method was used to synthesize statins loaded nanoemulsions. *In vitro*, atorvastatin and lovastatin loaded nanoemulsions were cytocompatible and were able to be uptake by oral epithelial cells. Treatment of *Porphyromonas gingivalis* infected oral epithelial cells and gingival fibroblasts with atorvastatin and lovastatin loaded nanoemulsions decreased significantly pro-inflammatory markers expression (TNF- α and IL-1 β) and pro-osteoclastic RANKL. Nevertheless, such treatment induced the expression of Bone sialoprotein 2 (BSP2) in osteoblast emphasizing the pro-healing properties of atorvastatin and lovastatin nanoemulsions. *In vivo*, in a calvarial bone defect model (2 mm), treatment with the hydrogel loaded with atorvastatin and lovastatin nanoemulsions induced a significant increase of the neobone formation in comparison with systemic administration of statins. This study demonstrates the potential of this statins loaded hydrogel to improve bone regeneration and to decrease soft tissue inflammation. Its use in the specific context of periodontitis management could be considered in the future with a reduced risk of side effects.

Keywords

hydrogel; periodontitis; *Porphyromonas gingivalis*; scaffold; atorvastatin; lovastatin

1.Introduction

Periodontitis is a chronic inflammatory disease of infectious origin characterized by a progressive destruction of tooth-supporting tissues including gingival tissues and alveolar bone (Pihlstrom *et al.*, 2005). Symptoms include gingival inflammation, periodontal pocket formation, clinical attachment and alveolar bone loss, abscess, tooth mobility and ultimately tooth loss. Periodontitis involves a complex interaction of immune and inflammatory cascades initiated by periodontal pathogens such as *Porphyromonas gingivalis* (*P.gingivalis*) associated to an exacerbated inflammatory host response (Hajishengallis, 2015). Currently, periodontal treatment, that consist of scaling and root planing, has a positive impact on periodontal health in most cases, however, it could be negatively influenced by the presence of systemic or local risk factors such as smoking or unadapted dental fillings sustaining the need of adjunctive therapies or surgical treatments (Graziani *et al.*, 2017) and the development of new pharmacological approaches (Akram *et al.*, 2017; Donos *et al.*, 2019; Gokhale and Padhye 2013; Martin-Cabezas *et al.*, 2016).

Several scaffolds for local delivery of active drugs and compounds have been developed. Such scaffolds should exhibit desirable biological and mechanical properties and should be easy-to use and cost-effective as well (Pina *et al.*, 2019). In this aspect, injectable scaffolds such as *in situ* forming implants (Batool *et al.*, 2019), membranes (Batool *et al.*, 2018) and gels (Joshi *et al.*, 2016) have been described. Indeed, chitosan hydrogel (ChiG), was already used successfully as an effective carrier to deliver drugs such as anti-inflammatory drugs and antibiotics within periodontal pocket (Akncbay *et al.*, 2007; Aminu *et al.*, 2019). Moreover, properties such as biocompatibility, low toxicity, biodegradability, antimicrobial and mucoadhesive properties render it an interesting scaffold in the context of periodontal treatment (Aguilar *et al.*, 2019; Sah *et al.*, 2019).

Statins, or inhibitors of 3-hydroxy-3-methylglutaryl coenzyme A reductase, are a group of drugs used primarily to treat hyperlipidemia and to prevent cardiovascular diseases (Mihaylova *et al.*, 2012). Recently, various pleiotropic properties of statins such as anti-inflammatory, antioxidant, antibacterial and immunomodulation properties have been described (Bedi *et al.*, 2016) allowing their use in the treatment of inflammatory diseases such as periodontitis (Petit *et al.*, 2019). Verily, statins reduce the pro-inflammatory cytokines levels (IL-1 β , IL-8, IL-6, TNF- α), increase the release of anti-inflammatory mediators (IL-10, IL-12) (Estanislau *et al.*, 2015; Grover *et al.*, 2016; Petit *et al.*, 2019) and have been demonstrated to regulate bone metabolism (Petit *et al.*, 2019; Zhang *et al.*, 2014). Moreover, statins have also displayed interesting antibacterial properties against key periodontal pathogens such as *P.gingivalis*, one of the major pathogens detected in deep periodontal lesions (Emani *et al.*, 2014; Lee *et al.*, 2016a). In the context of periodontal treatment, several clinical trials have demonstrated a beneficial effect of adjunctive systemic statin administration on non-surgical periodontal treatment response (Fajardo *et al.* 2010; Fentoğlu *et al.* 2012). However, the risk of side effects associated to the administered dose led to the development of local administration strategy including dentifrice and gels (Muniz *et al.*, 2018). Interestingly, their local application, as an adjunct to the mechanical debridement, induced greater reduction of periodontal probing depth, depth of the radiographic defect and bleeding index compared to the outcomes obtained when statins were systemically administered demonstrating the importance of the route of administration (Muniz *et al.*, 2018).

Several statins have been evaluated to promote periodontal healing. Notably, simvastatin, atorvastatin and rosuvastatin presented their beneficial properties to enhance periodontal regeneration and to decrease the production of pro-inflammatory cytokines in several *in vitro*, *in vivo* and clinical studies (Fajardo *et al.*, 2010; Kırzioğlu *et al.*, 2017;

Pradeep *et al.*, 2015; Rao *et al.*, 2013; Sousa *et al.*, 2016; Thylin *et al.*, 2002). Although simvastatin was the most studied statin for its advantageous effect on periodontal regeneration, atorvastatin and lovastatin have shown identical and sometimes superior effects on bacterial clearance, bone metabolism, immune and inflammatory responses (de Araújo Júnior *et al.*, 2013; Ko *et al.*, 2017; Subramanian *et al.*, 2013; Weitz-Schmidt *et al.*, 2001). Indeed, in a randomized clinical trial, Pradeep *et al.*, showed that the local administration of 1.2% atorvastatin gel as adjunctive to scaling and root planing improved treatment outcomes. However, the adjunctive effects measured was lower than those observed for the local administration of a 1% alendronate containing gel (Pradeep *et al.*, 2016). Interestingly, a recent meta-analysis, showed that all statins do not induce the same clinical outcomes emphasizing the need of specific evaluation of all types of statins (Muniz *et al.*, 2018). Since atorvastatin and lovastatin, two lipophilic statins, are insoluble in aqueous solution, their formulation and dispersion in the aqueous matrix of such hydrogels is crucial for allowing stability and bioavailability (Yang *et al.*, 2018). For this purpose, nanoemulsions are considered very adapted for the local delivery of lipophilic active compounds (Anton and Vandamme, 2009; Anton *et al.*, 2016). They consist of a dispersion of oily droplets – able to solubilize lipophilic molecules- in an aqueous phase, sizing below 300 nm (Ganta *et al.*, 2010) and stabilized by surfactants, generally nonionic surfactants, such as D- α -Tocopherol polyethylene glycol succinate (TPGS), a water-soluble derivative of natural vitamin E (Zhang *et al.*, 2012). The use of nanoemulsions also allows to increase the concentration of the active drug in a given volume and to facilitate the uptake by the target cells compared to ordinary drug-carrying gels (Martínez-Ballesta *et al.*, 2018).

The aim of this study was to synthesize, characterize and evaluate, *in vitro* and *in vivo*, the potential anti-inflammatory and pro-regenerative effects of a thermosensitive ChiG functionalized by atorvastatin TPGS nanoemulsions and lovastatin TPGS nanoemulsions.

2. Materials & Methods

2.1 Synthesis of thermosensitive chitosan-based hydrogel (ChiG)

2.5% chitosan solution was prepared by dissolving 125 mg of chitosan (MW: 50 000-190 000 Da; 75-85% deacetylated) (Sigma-Aldrich, St-Quentin, France) in 5 ml of a 1% aqueous acetic acid solution. After cooling the chitosan solution to 4°C, 600 mg of glycerophosphate (Gp) salt powder (Sigma-Aldrich) was added. This concentration of Gp at 0.56M ensures a thermo-irreversible gelification at 37°C. The mixture was maintained for 15 min with constant stirring. The resulting transparent ChiG solution was stored at 4°C before injection (Ganji *et al.*, 2007; Madi and Kassem, 2018).

2.2 Solubility test for atorvastatin and lovastatin

Since atorvastatin (Sigma-Aldrich) and lovastatin (Sigma-Aldrich), two lipophilic statins, display low solubility in chitosan, solubilizer must be added to the mixture. The solubility of atorvastatin and lovastatin was tested in 7 surfactant or co-surfactant oils: kolliphor ELP (BASF, Ludwigshafen, Germany), capmul MCM C8 (Abitec, Columbus, USA), castor oil (Sigma-Aldrich, Saint Louis, USA), labrafil M 1944 CS (Gattefossé, Saint Priest, France), tetraglycol (Sigma-Aldrich), transcitol P (Gattefossé) and TPGS (Sigma-Aldrich). 2 mg of atorvastatin and lovastatin were mixed with 1 ml of tested surfactant or co-surfactant before being vortexed for 30 s, passed through an ultrasonic bath for 5 min and then heated at 80°C for 5 min. If a one-phase clear solution was obtained, the addition of atorvastatin and lovastatin was repeated until the solution became cloudy. Finally, TPGS was chosen as it allowed the solubilization of a higher concentration of atorvastatin and lovastatin in the tested liquid volume. Then, the solubility of atorvastatin and lovastatin was evaluated in TPGS, MEtOH in milliQ water (50:50) and in milliQ water. Briefly, 2-20 µg/ml were dissolved in 1 ml of each solution, heated 5 min at 80°C, sonicated for 5 min and vortexed for

30 s. Solubilized atorvastatin and lovastatin were measured using a spectrophotometer (UviLine 9100, Secomam) at 246 nm for atorvastatin and 248 nm for lovastatin.

2.3 Formulation of nanoemulsions by spontaneous emulsification

The nanoemulsions were prepared according to a low-energy process, so-called spontaneous nano-emulsification method. This low-energy formulation process is rapid, easy to handle, prevents the degradation of fragile drugs and is free from the toxicity of organic (Anton, Benoit, and Saulnier 2008). The solubilization of atorvastatin and lovastatin in an equal mixture of vitamin E acetate (TCI chemicals, Portland, USA) and TPGS (50:50) resulted in the formation of an organic solution. Then, the oil-surfactant-statin mixture was gently warmed until 80°C before a sudden injection of an aqueous phase (distilled water) at 25°C. The mixture is then gently mixed, *ca.* one minute, up to a homogeneous solution is obtained. This experiment was repeated with the addition of an increased amount of distilled water until the maximum water solubilization capacity (W_{max}) was determined visually by the passage from a transparent NE formulation to a cloudy mixture. W_{max} was reached with a water/oil-surfactant-statin ratio of 80:20. This ratio was selected for the synthesis of nanoemulsions containing atorvastatin (20 g/L) or lovastatin (20 g/L).

2.4 Transmission electron microscopy (TEM)

To determine nanoemulsions size and morphology, nanoemulsions were observed under TEM. A droplet of atorvastatin TPGS nanoemulsions and lovastatin TPGS nanoemulsions were placed on carbon-coated TEM copper grids (Sigma-Aldrich) and left to air-dry. Then, a droplet of an aqueous solution of uranyl acetate (2% wt) (Merck, Darmstadt, Germany) was added. The grid was then air-dried before being viewed using TEM (TEM FEI Technai F30 and probe aberration corrected FEI-Titan 60-300).

2.5 Particles size, distribution and zeta potential analysis

Nanoemulsions size distribution (measured by dynamic light scattering (DLS)) and zeta potential values (measured by electrophoretic light scattering) were assessed using a Malvern NanoZS instrument (Malvern, Orsay, France). The helium-neon laser (4 mW) operates at 633 nm with the scatter angle fixed at 173° at 25°C.

2.6 Release study

500 µL of ChiG with atorvastatin TPGS nanoemulsions and lovastatin TPGS nanoemulsions were deposited in each well of a 6-well plate. Then, the plate was heated for 10 min at 40°C to induce gelification. Finally, 10 mL of distilled water were added to each well of the 6-well plate maintained with constant agitation. 700 µL of each sample were collected at regular time intervals for 24h to determine released atorvastatin TPGS nanoemulsions and lovastatin TPGS nanoemulsions concentration against a standard range curve using UV spectrophotometry (246 nm for atorvastatin and 248 nm for lovastatin) (UviLine 9100, Secomam). pH was measured using an electronic pH meter (H 15221, Hanna instruments, USA).

2.7 Cell metabolic activity

TERT-2 OKF-6 Human Oral Epithelial Cells (EC) (BWH Cell Culture and Microscopy Core, Boston, MA, USA) were cultured in Keratinocyte-SFM medium (Life Technologies, Fisher Scientific, Illkirch, France) supplemented with a mixture of growth supplements and antibiotics (10 U/ml penicillin and 100 µg/ml streptomycin) (Lonza, Levallois-Perret, France). Human oral fibroblasts (FB) were isolated from gingival biopsy (French Ministry of Research, authorization DC-2014-2220) and cultured in RPMI 1640 medium supplemented with 10% fetal bovine serum (Life Technologies), 2 mM glutamine,

250 U/ml fungizone and antibiotics (10 U/ml penicillin and 100 µg/ml streptomycin). Cryopreserved primary human osteoblasts (OB) C-12720 isolated from femoral trabecular bone tissue (PromoCell, Heidelberg, Germany) were cultured in osteoblast-SFM medium (Life Technologies) supplemented with a mixture of growth supplements and antibiotics (10 U/ml of penicillin and 100 µg/ml of streptomycin) (Lonza). The cells were cultured at 37°C in a humidified atmosphere with 5% CO₂ and the culture medium was changed every 2 to 3 days.

Metabolic activity was determined using colorimetric AlamarBlue test (Life Technologies). Twenty-four hours before the experiment, 2x10⁵ cells were seeded in each well of a 24-well plate. At the day of the experiment, EC, FB and OB were washed twice with PBS and treated with cell media containing 5 or 10 µM of atorvastatin TPGS nanoemulsions or lovastatin TPGS nanoemulsions. After 24h, EC, FB and OB were washed twice with PBS and incubated with cell media containing 10% of AlamarBlue cell viability reagent for 4h. Then, 300 µL of incubation media were transferred to 96-well plates and measures at OD₅₇₀ and OD₅₉₅ nm with a spectrophotometer (Multiskan, ThermoScientific, Illkirch, France) were performed in order to determine the percentage of AlamarBlue reduction.

2.8 Bacterial culture and infection

The *P.gingivalis* strain ATCC 33277 was purchased from the American Type Culture Collection (ATCC, Manassas, VA, USA). Bacterial culture was performed under strict anaerobic conditions at 37°C in Brain-Heart Infusion medium supplemented with hemin (5 µg/ml) and menadione (1 µg/ml) (Sigma-Aldrich). Twenty-four hours before the experiment, 2x10⁵ cells were plated in each well of a 24-well plate. At the day of the experiment, EC and FB were washed twice with PBS and infected for 24h with *P.gingivalis* at a multiplicity of infection (MOI) of 100 bacteria/cell.

2.9 Nanoemulsions cellular uptake

The endocytic capacity of atorvastatin TPGS nanoemulsions and lovastatin TPGS nanoemulsions was evaluated in EC. 2×10^5 cells per well were seeded in a 24-well plate. After 24h, a NR668-labeled (1% wt. in oil) atorvastatin TPGS nanoemulsions (10 μ M) and lovastatin TPGS nanoemulsions (10 μ M) solution diluted in the cell culture medium replaced the culture medium of each well after thorough rinsing with PBS. The custom-made fluorescent NR668 is a lipophilic version of Nile Red, which is very stable inside the nanoemulsion droplets. Thus, the droplets are colocalized with the dye and can be tracked by fluorescence (Klymchenko *et al.*, 2012). Fluorescence was observed after 24h with a fluorescent microscope (Leica DM 4000B).

2.10 RNA Isolation, Reverse Transcription and Quantitative Real-Time PCR Analysis

To assess, mRNA expression of TNF- α , IL-1 β and RANKL, RT-qPCR was performed. Total RNA was extracted using TRIzol reagent (Invitrogen) according to the manufacturer's instructions. RNA concentrations and purity were determined using the NanoDrop ND-1000 spectrophotometer (NanoDrop Technologies, Rockland, DE, USA). Reverse transcription was performed with the iScript Reverse Transcription Supermix (Bio-Rad Laboratories, Hercules, CA, USA) according to the manufacturer's instructions. To quantify RNA expression, qPCR was performed on the cDNA samples. PCR amplification and analysis were achieved using the CFX Connect™ Real-Time PCR Detection System (Bio-rad, Miltry-Mory, France). Amplification reactions have been performed using iTaq Universal SYBR Green Supermix (Bio-rad). All primers used for this study are listed in Table 1. Validated PCR primers pairs for the human TNF- α and IL-1 β (purchased from Invitrogen) and human gene RANKL (purchased from Eurofins Scientific, Luxembourg) were used at the

final concentration recommended by the respective manufacturers. The specificity of the reaction was controlled using melting curves analysis. The expression level was calculated using the comparative Ct method ($2^{-\Delta\Delta C_t}$) after normalization to the housekeeping gene β -actin (Invitrogen). All PCR assays were performed in triplicate and results were represented by the mean values and SD.

Gene		Primer sequence
β -actin	Forward	GATGAGATTGGCATGGCTTT
	Reverse	GACCTTCACCGTTCCAGTTT
IL1- β	Forward	TCCCCAGCCCTTTTGTGA
	Reverse	TTAGAACCAAATGTGGCCGTG
TNF- α	Forward	GCCTCTTCTCCTTCCTGATCGT
	Reverse	CTCGGCAAAGTCGAGATAGTCG
RANKL	Forward	GCCAGTGCCAGATGTTAG
	Reverse	TTAGCTGCAAGTTTTCCC

Table 1: List of primers used in this study

2.11 Immunofluorescence staining of bone sialoprotein 2 (BSP2) in OB

OB were cultured on round glass and treated with 10 μ M of atorvastatin, lovastatin, atorvastatin TPGS nanoemulsions or lovastatin TPGS nanoemulsions. After 1 day of culture in respective media, cells were fixed with 4% paraformaldehyde during 10 min at 37°C. The samples were rinsed 3 times with PBS and incubated in 0.1% (v/v) of Triton X-100 and bovine serum albumin (BSA) 1% (m/v). Indirect immunostaining was performed after the fixation. The primary antibody used was the mouse monoclonal IgG1 human anti-BSP2 (Santa Cruz Biotechnology, TX, USA) (1/200) incubated overnight at 4°C. The secondary antibody was 594 Alexa Fluor donkey anti-mouse IgG (Molecular Probes; Life Technologies, Fisher Scientific, Illkirch, France) (1/500) incubated during 2h. PBS rinses were made and phalloidin (Alexa Fluor 488, Thermofisher) (1/100) was added during 20 min at room temperature. A DAPI (Sigma-Aldrich) solution (200 nM) was then added for 5 min to achieve nuclear staining. After mounting with Dako (Dako, Courtaboeuf, France), the samples were observed with an epifluorescent microscope (Leica DM 4000B).

2.12 Treatment of calvarial bone defect

All experiments were performed with the approval of the Veterinary Public Health Service of the Préfecture du Bas-Rhin, representing the French Ministry of Agriculture, Department of Veterinary Science (APAFIS#23885-2020013114423121v3). This experimental protocol fulfilled the authorization of the “Ministère de l’Enseignement Supérieur et de la Recherche”. The Ethics Committee of Strasbourg named “Comité Régional d’Ethique en Matière d’Expérimentation Animale de Strasbourg (CREMEAS)” specifically approved this study. To avoid any potential effects of estrogen, 8 weeks old male mice C57BL/6J (Janvier Labs, Le Genest-Saint-Isle, France) were used in this study.

The mice were anesthetized intraperitoneally with a mixture of ketamine (80 mg/kg) and xylazine (10 mg/kg). Calvarial defect was performed as described previously (Keller *et al.*, 2017). Briefly, the head was shaved before making a single vertical incision in the middle of the skull until bone contact. The calvarial defect (500 µm deep and 2 mm in diameter) was drilled in the parietal zone of the skull using a sterile round bur, under irrigation of sterile saline solution. After cleaning the surgical wound with physiological saline and drying by tamponade, a drop of 50 µL of atorvastatin TPGS nanoemulsions ChiG (2 g/L), lovastatin TPGS nanoemulsions ChiG (2 g/L), atorvastatin ChiG (2 g/L), lovastatin ChiG (2 g/L) or ChiG (4 mice/group) were deposited in the calvarial defect. Finally, a continuous suture (resorbable suture 6-0, SAFIL[®], B Braun Surgical SA, Rubi, Spain) was performed to allow primary wound closure. To compare with systemic administration, atorvastatin and lovastatin were also administered by oral gavage (10 mg/kg/day) for 15 days. Two weeks after the surgery, mice were sacrificed with pentobarbital injection (100 mg/kg) (Centravet, Nancy, France) (Figure 1).

2.13 *In vivo* calcein injection

Injections of calcein in PBS (10 mg/kg, Sigma-Aldrich) were performed subcutaneously on mice, at day 5 and day 12 to detect the formation of new bone tissue. This fluorescent compound will bind to Ca^{2+} ions in blood circulation and, simultaneously, it will be incorporated into the newly formed bone (Keller *et al.*, 2017).

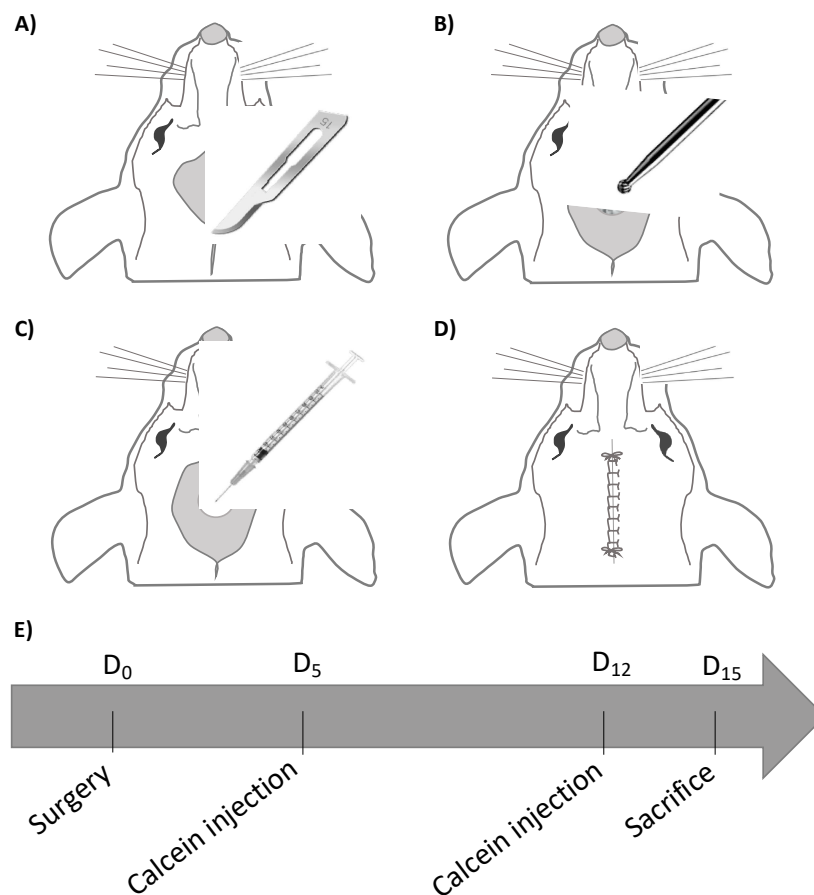


Figure 1: Surgical preparation of calvarial defect (2 mm) and ChiG application. A) A single vertical incision was first made in the middle of the skull. B) A bone defect was carefully created by drilling with a round bur using constant irrigation to avoid bone over-heating. The defect was cleaned with physiological saline, dried with a gauze and C) treated with local application of atorvastatin TPGS nanoemulsions ChiG, lovastatin TPGS nanoemulsions ChiG, atorvastatin ChiG, lovastatin ChiG, ChiG or left untreated. D) The wound was finally

sutured hermetically with 6.0 suture. E) Calcein was injected 10 and 3 days before sacrifice to determine neo-bone formation.

2.14 Tissue preparation

The calvaria were dissected and fixed for one day by immersing in a solution of 4% paraformaldehyde (PFA) diluted in PBS. After washing in PBS, the samples were embedded in Optimal cutting temperature compound OCT Tissue Tek® (Optimum Cutting Temperature; Fisher Scientific, France) and frozen. Then, 10 µm thick serial sections were cut from each sample with a cryostat (Leica CM 3000) at -25°C.

2.15 Histological and immunofluorescence analyses

Half of the sections were immersed for 10 min in PFA before being rinsed and stained for 5 min in alizarin red (Sigma-Aldrich). Slides were mounted using DAKO mounting medium prior to examination under microscope (RM 2145 DMRB microscope, Leica, Rueil-Malmaison, France). Other half sections were dipped 10 min in PFA before being rinsed and stained for 5 min in 200 nM DAPI solution (Sigma-Aldrich) to stain cell nuclei. Sections were then mounted and examined under fluorescence microscope. The immunofluorescent calcein staining was followed using fluorescent microscope (RM 2145 DMRB microscope, Leica, Rueil-Malmaison, France). The circumference of neo-bone area was marked and measured by Olympus cellSens Entry imaging software. At least 3 samples per mouse were considered for each condition.

2.16 Statistical analysis

All experiments were repeated at least three times in triplicates (technical and biological replicates), and statistical analysis was performed using ANOVA and Mann Whitney U test using Prism 8.0 software (GraphPad, La Jolla, CA, USA). A p -value < 0.05 was considered significant.

3. Results

3.1 Characterization of nanoemulsions and nanoemulsions loaded ChiG

Morphology of the synthesized nanoemulsions was evaluated by TEM analysis (Table 2). All nanoemulsions exhibited a spherical morphology with a diameter between 40 nm and 200 nm (mean=137 nm for atorvastatin TPGS nanoemulsions and 169 nm for lovastatin TPGS nanoemulsions) (Figure 2A, 2B, 2D, 2E; Table 2). The nanoemulsions surface charge was on average -29 mV (atorvastatin TPGS nanoemulsions) and -18.5 mV (lovastatin TPGS nanoemulsions) (Figure 2C and 2F). All synthesized ChiG loaded and non-loaded with atorvastatin TPGS nanoemulsions and lovastatin TPGS nanoemulsions had a pH between 6.3 and 6.8, thus, potentially cytocompatible.

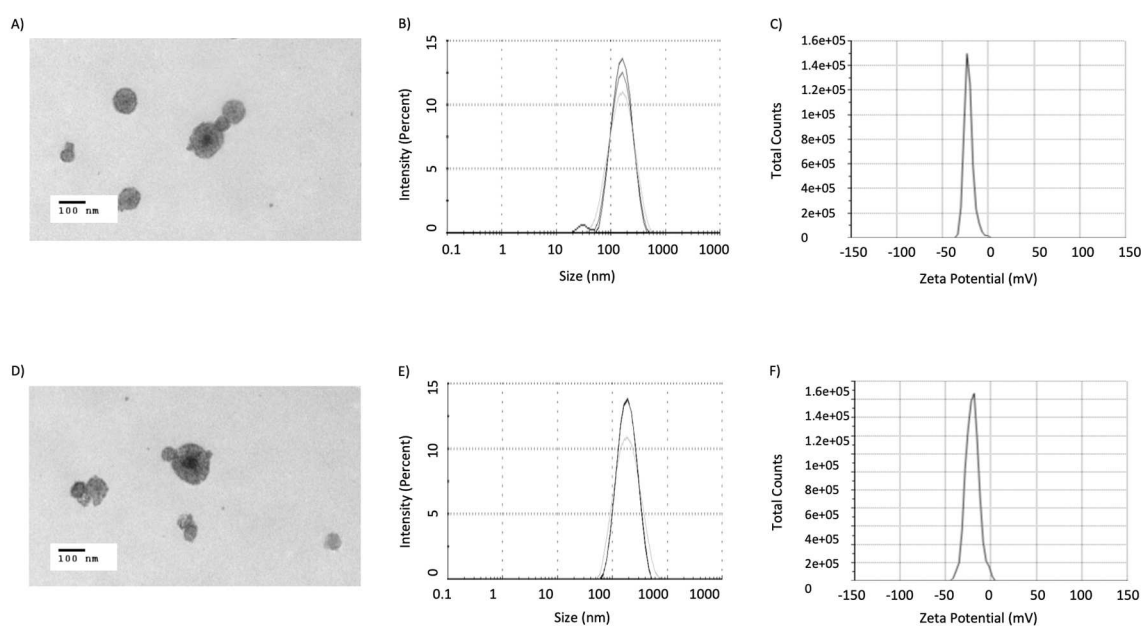


Figure 2: Analysis of droplet size and surface charge of atorvastatin TPGS nanoemulsions and lovastatin TPGS nanoemulsions. For TEM, the samples with atorvastatin TPGS nanoemulsions (A) and lovastatin TPGS nanoemulsions (D) were labeled with uranyl acetate. Average size of atorvastatin TPGS nanoemulsions was 137.3 nm (B) and 169.2 nm for

lovastatin TPGS nanoemulsions (E). The surface charge of atorvastatin TPGS nanoemulsions (C) and lovastatin TPGS nanoemulsions (F) was assessed using the Zetasizer device.

Nanoemulsion characteristics		ATV TPGS	LOVA TPGS
Size and size distribution	Z-Average size (d.nm)	137.3	169.2
	SD (d.nm)	73.18	78.72
	Polydispersity Index (PDI)	0.183	0.141
	PDI Width	58.73	63.53
Surface charge	Zeta potential (mV)	-29m	-18.5
	Zeta deviation (mV)	4.38	4.98
	Conductivity (mS/cm)	0.00901	0.0713
	Effective voltage (V)	148.4	147.8

Table 2: Nanoemulsions characteristics. ATV TPGS: atorvastatin TPGS nanoemulsion; LOVA TPGS: lovastatin TPGS nanoemulsions; SD: standard deviation.

3.2. Solubility of atorvastatin and lovastatin

To determine the interest of TPGS nanoemulsions, solubility of atorvastatin and lovastatin was evaluated (Figure 3). Solubility in TPGS was 50% higher for both statins than in MEtOH ($p < 0.05$).

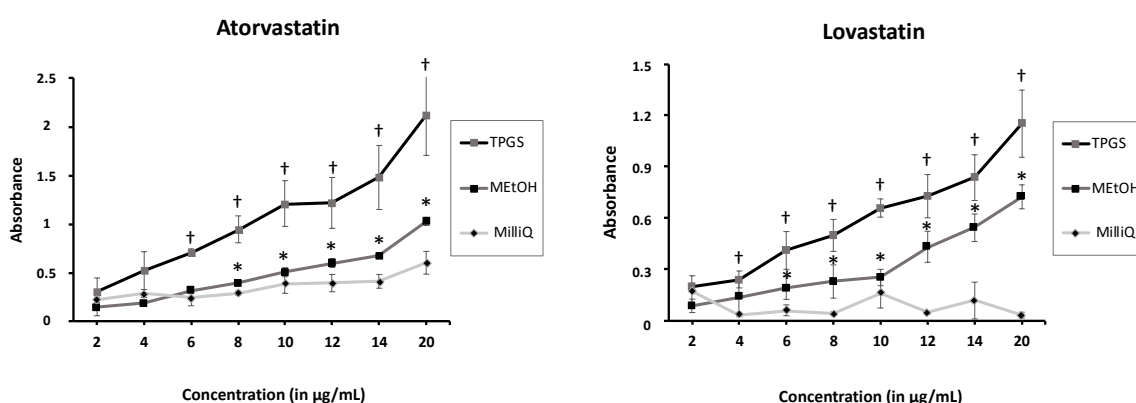


Figure 3: Solubility of atorvastatin and lovastatin. 2 to 20 µg of atorvastatin and lovastatin were solubilized in TPGS, MEtOH (50:50) and milliQ water (MilliQ). Absorbance at 246 nm

(atorvastatin) and at 248 nm (lovastatin) was measured. † Difference between TPGS and other conditions, $p < 0,05$. * Difference between MEtOH and MilliQ, $p < 0,05$.

3.2 In vitro drug release

Figure 4 shows the *in vitro* release of atorvastatin and lovastatin TPGS nanoemulsions from ChiG in water. The release from the ChiG follows a linear curve with a coefficient of determination greater than 0.95. At 24h, about more than 70% of the atorvastatin and lovastatin loaded TPGS nanoemulsions were released from ChiG.

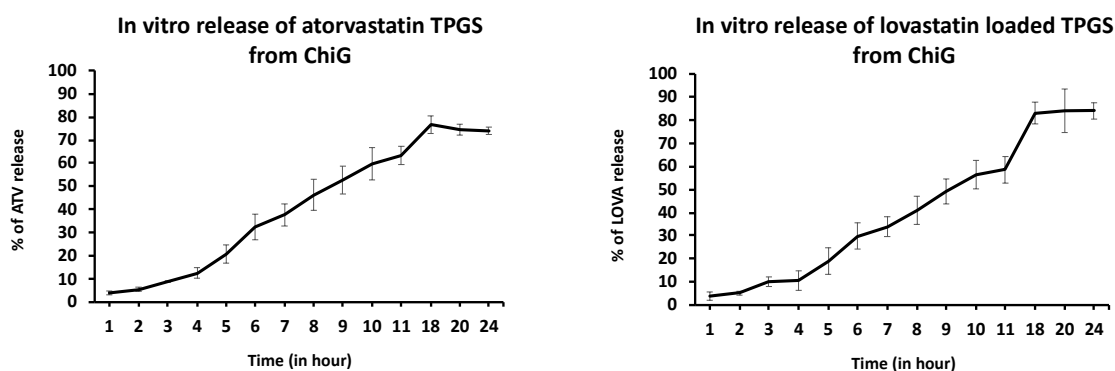


Figure 4: *In vitro* release of atorvastatin and lovastatin loaded TPGS from ChiG. ChiG containing atorvastatin and lovastatin loaded TPGS nanoemulsions was injected in a 6-wells plate and release of atorvastatin and lovastatin loaded TPGS nanoemulsions in water was measured during 24h with UV spectrophotometer.

3.3 Cytocompatibility of atorvastatin and lovastatin loaded TPGS nanoemulsions

To evaluate the cytocompatibility of atorvastatin TPGS nanoemulsions and lovastatin TPGS nanoemulsions, the metabolic activity of EC, FB and OB was evaluated. Cells were incubated 24h with 5 or 10 μM of atorvastatin TPGS nanoemulsions or lovastatin TPGS

nanoemulsions. No significant modification of metabolic activity was measured after cells' exposure ($p < 0.05$) for all tested cell types (Figure 5).

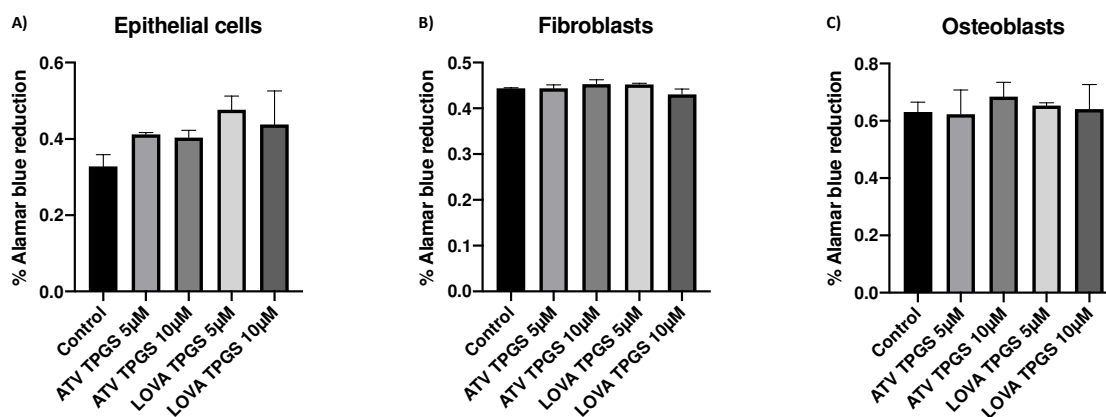


Figure 5: Metabolic activity of epithelial cells, fibroblasts and osteoblasts. A) EC metabolic activity. B) FB metabolic activity. C) OB metabolic activity. Cells were treated by atorvastatin TPGS nanoemulsions 5 or 10 μM and lovastatin TPGS nanoemulsions 5 or 10 μM for 24h; data were expressed as the mean \pm SD. No significant differences were found between Control (untreated cells) and other conditions ($p > 0.05$).

3.4 Evaluation of atorvastatin TPGS nanoemulsions and lovastatin TPGS nanoemulsions cellular uptake

As statins have an intra-cellular mode of action, the cellular uptake capacity of atorvastatin TPGS nanoemulsions and lovastatin TPGS nanoemulsions was evaluated in EC (Figure 6). After 24h, an intra-cytoplasmic localization of the fluorescent NR668 loaded within atorvastatin TPGS nanoemulsions and lovastatin TPGS nanoemulsions was observed confirming the ability of TPGS nanoemulsions to be uptaken and to deliver the active drug.

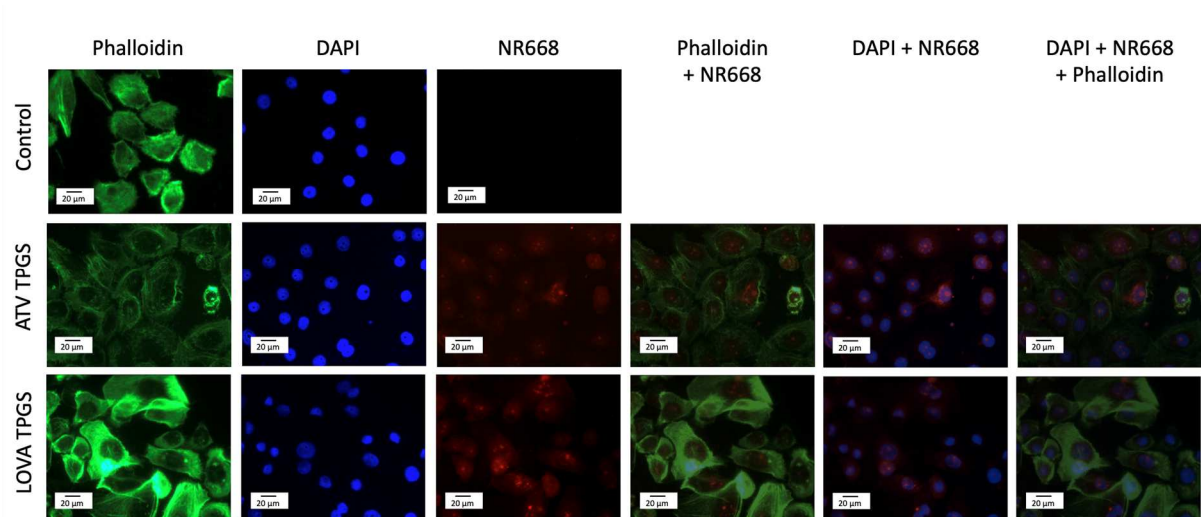


Figure 6: Cellular uptake of atorvastatin TPGS nanoemulsions and lovastatin TPGS nanoemulsions. NR668 dye was added to atorvastatin TPGS nanoemulsions (ATV TPGS) and lovastatin TPGS nanoemulsions (LOVA TPGS). EC were treated with atorvastatin TPGS nanoemulsions (10 μ M) and lovastatin TPGS nanoemulsions (10 μ M) for 24h at 37°C. After incubation, the internalization of the NR668 dye (red) in the cytoplasm confirms the cellular uptake of atorvastatin TPGS nanoemulsions and lovastatin TPGS nanoemulsions (green: phalloidin; blue: DAPI – nuclear staining; red: NR668 dye). Control: untreated cells. Magnification was 40x.

3.5 Anti-inflammatory and anti-resorptive effects of atorvastatin TPGS nanoemulsions and lovastatin TPGS nanoemulsions

To evaluate the anti-inflammatory and anti-resorptive effects of atorvastatin TPGS nanoemulsions and lovastatin TPGS nanoemulsions on pro-inflammatory factors, EC and FB were infected with *P.gingivalis* and treated for 24h with atorvastatin TPGS nanoemulsions and lovastatin TPGS nanoemulsions. Relative gene expression for TNF- α , IL-1 β and RANKL was measured (Figure 7). As expected, *P.gingivalis* infection increased significantly TNF- α , IL-1 β and RANKL expression ($p < 0.05$) in EC and FB. Treatment with atorvastatin TPGS nanoemulsions and lovastatin TPGS nanoemulsions decreased significantly the gene

expression of all above-mentioned markers in EC ($p < 0.05$). In FB, a significant effect was observed for TNF- α while a decreasing trend was shown for IL-1 β and RANKL expression.

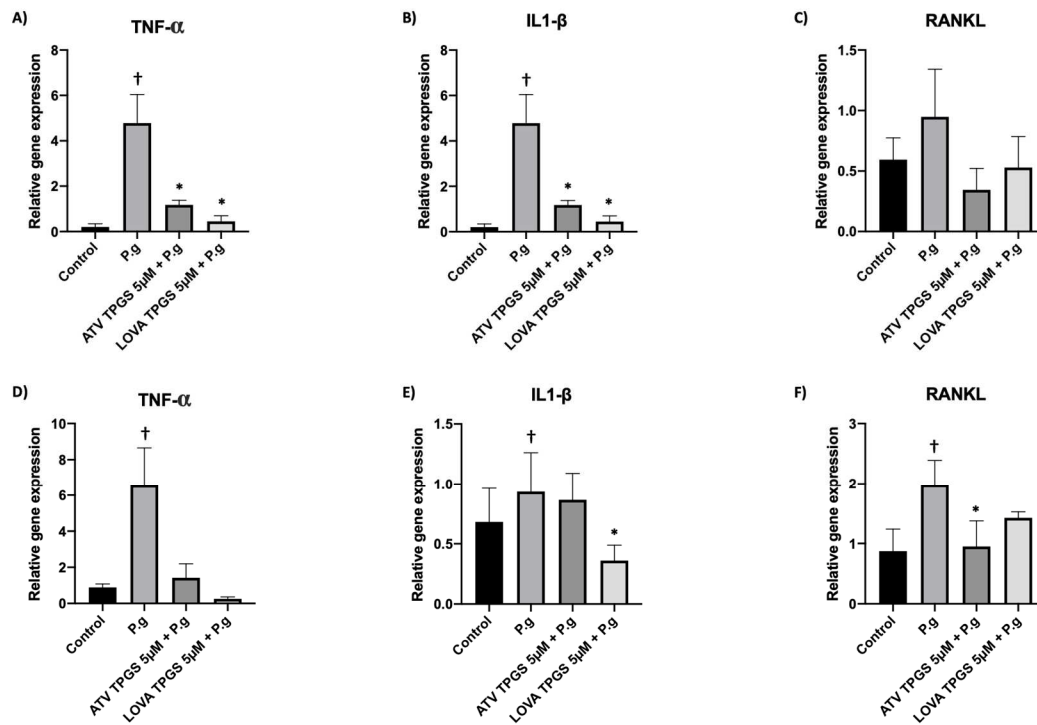


Figure 7: Gene expression of TNF- α , IL-1 β and RANKL. Cells were infected for 24h with *P.gingivalis* (MOI=100) and treated 24h with atorvastatin TPGS nanoemulsions (ATV TPGS) (10 μ M) and lovastatin TPGS nanoemulsions (LOVA TPGS) (10 μ M). Relative mRNA levels were analyzed by real-time RT-qPCR in EC (A), (B), (C) and FB (D), (E), (F). Data are expressed as mean \pm SD. † Difference between non-stimulated and stimulated cells, $p < 0.05$. * Difference between atorvastatin TPGS nanoemulsions or lovastatin TPGS nanoemulsions treated cells stimulated with *P.gingivalis* (P.g) and non-treated cells stimulated with *P.gingivalis*, $p < 0.05$. Control: untreated cells.

3.6 Evaluation of the osteogenic effect of atorvastatin TPGS nanoemulsions and lovastatin TPGS nanoemulsions

To evaluate the osteogenic properties of atorvastatin TPGS nanoemulsions and lovastatin TPGS nanoemulsions, OB were treated for 24h (Figure 8). The expression of BSP2,

a significant component of the bone extracellular matrix, was qualitatively evaluated by immunofluorescence microscopy. After 24h of OB treatment, a slight increase of BSP2 expression was observed in atorvastatin and lovastatin treated cells. Interestingly, BSP2 expression was significantly increased in atorvastatin TPGS nanoemulsions and lovastatin TPGS nanoemulsions treated cells emphasizing the positive effect of TPGS nanoemulsions as statin carrier.

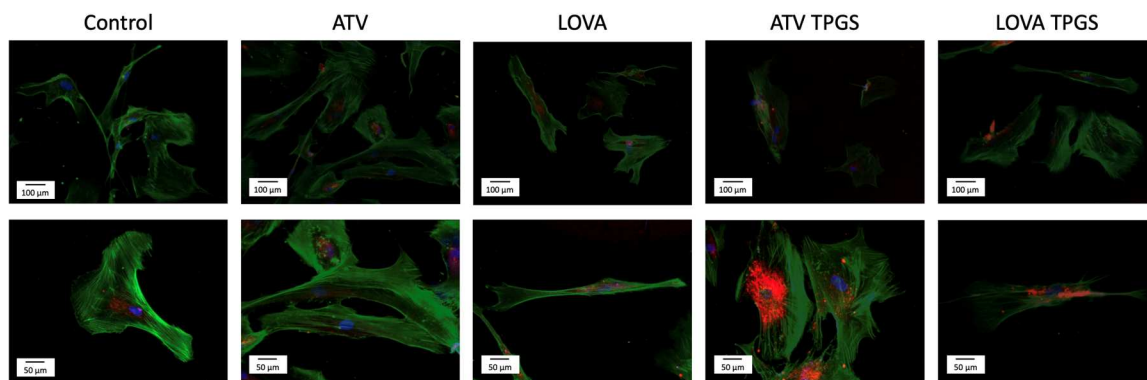


Figure 8: Expression of BSP2 in OB. Cells were treated for 24h with atorvastatin TPGS nanoemulsions (ATV TPGS) (10 μ M) and lovastatin TPGS nanoemulsions (LOVA TPGS) (10 μ M) for 24h at 37°C. After treatment, a significant increase of BSP2 expression was observed in atorvastatin TPGS nanoemulsions (10 μ M) and lovastatin TPGS nanoemulsions (10 μ M) in comparison with atorvastatin (ATV) (10 μ M) and lovastatin (LOVA) (10 μ M) treated cells (green: phalloidin; blue: DAPI – nuclear staining; red: BSP2). Control: untreated cells. Magnification was 10x and 20x.

3.7 Statins functionalized nanoemulsions induce neo-bone formation in vivo

Atorvastatin TPGS nanoemulsions ChiG and LOVA TPGS nanoemulsions ChiG was injected in standardized (2 mm) calvarial bone defect. Early signs of calcification and neo-bone formation were evaluated 2 weeks after ChiG treatment and compared to atorvastatin and lovastatin systemic administration (Figure 9) to evaluate its therapeutic

potential *in vivo*. During the procedures and follow-up, neither significant weight changes nor any adverse events were observed. After 15 days, the calcein stained area was measured in all groups. Amongst all tested groups, lesions treated with lovastatin ChiG, atorvastatin TPGS nanoemulsions ChiG and lovastatin TPGS nanoemulsions ChiG exhibited a significant increase of neo-bone formation confirmed by the presence of speckled areas of new bone within the defect area. Interestingly, the most significant bone healing effect was observed in atorvastatin TPGS nanoemulsions ChiG and lovastatin TPGS nanoemulsions ChiG demonstrating the interest of TPGS nanoemulsions to deliver efficiently the active drugs. Nevertheless, the soft tissue surrounding atorvastatin TPGS nanoemulsions ChiG and lovastatin TPGS nanoemulsions ChiG treated lesions showed decreased inflammation characterized by reduced inflammatory cellular infiltration when compared to the other tested conditions. However, due to short term of follow-up, no significant differences were observed in terms of a decrease in the lesion length.

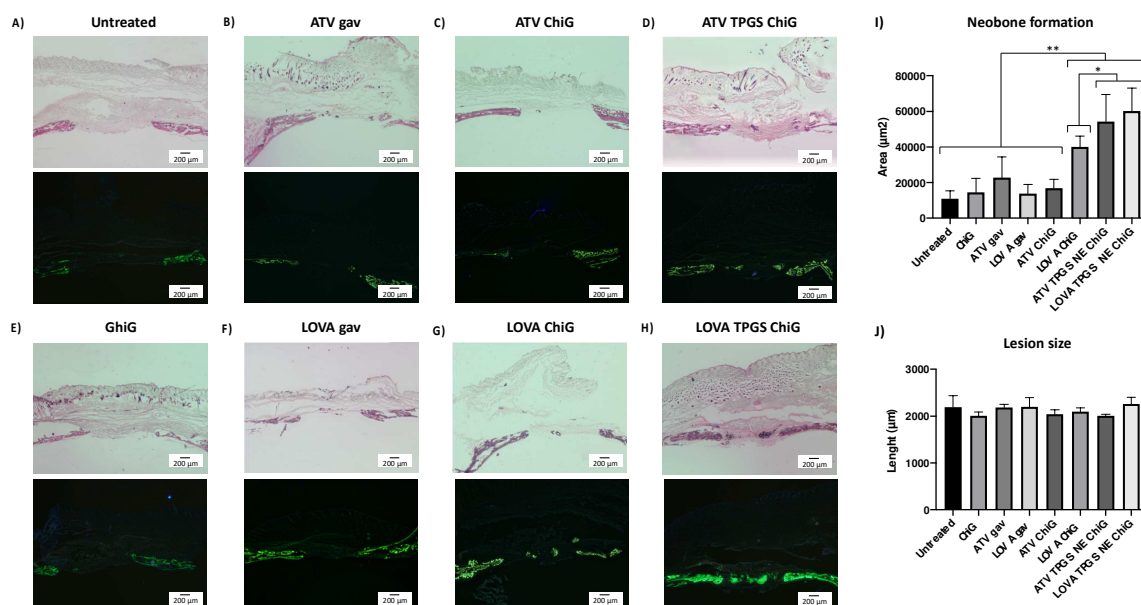


Figure 9: Histological and corresponding immunofluorescent sections of induced bone defect after 15 days of wound healing (A-H) and histomorphometric analysis of histological

sections. *Histological view at 15 days stained with alizarine red (upper images) or calcein (lower images) of (A) untreated, (B) atorvastatin gavage (ATV gav), (C) atorvastatin ChiG, (D) atorvastatin TPGS nanoemulsions ChiG, (E) ChiG, (F) lovastatin gavage (LOVA gav), (G) lovastatin ChiG (LOVA ChiG) and (H) lovastatin TPGS nanoemulsions ChiG. Histomorphometric analysis of neobone formation (I) and lesion size (J) after 15 days. Data are expressed as mean \pm SD. *, $p < 0.05$; **, $p > 0.001$*

4. Discussion

Statins have been suggested as potentially effective pro-regenerative drugs due to their pleiotropic properties (Petit *et al.*, 2019). They modulate several physiological pathways involved in both inflammatory-immune crosstalk and bone metabolism resulting in the reduction of inflammatory markers expression, osteoclastogenesis, bone resorption and increase osteogenesis (Bertl *et al.*, 2017; Zhang *et al.*, 2014). However, the improvement in bone regeneration induced by statins *in vivo* depends on the local concentration of the drug (Zhang *et al.*, 2014). In this study, we designed a chitosan based hydrogel and demonstrated the efficiency of atorvastatin TPGS nanoemulsions ChiG and lovastatin TPGS nanoemulsions ChiG to reduce *P.gingivalis*-elicited inflammation *in vitro* and to promote bone healing in an *in vivo* model of induced calvarial defect.

In periodontal regeneration, the use of cost-effective and easy-to-handle scaffold is of importance. Local drug delivery system into periodontal pockets offers many advantages, namely improvement of patient compliance, reduction of treatment cost, safer route of drug administration, limitation of dose due to bypass of first-pass metabolism by the liver, thereby, decreasing the risk of side effects (Joshi *et al.*, 2016). Therefore, the use of gels, especially hydrogels, will be of interest as they are easy to inject directly inside the periodontal lesion. Hydrogels display the ideal scaffold characteristics. They are biocompatible, biodegradable and exhibit a 3D structure similar to the natural cellular environment (Nagy *et al.*, 2018; Pina *et al.*, 2019). In this study, chitosan hydrogel was selected. Chitosan is a natural multifunctional polysaccharide highly biocompatible, biodegradable with muco-adhesive properties (Aguilar *et al.*, 2019). It is used to synthesize different types of scaffold including fibrous scaffolds and hydrogels (Sah *et al.*, 2019) and is already used for local drug administration owing to its properties such as mechanical strength, strong adhesion to tooth surface, injectability. Indeed, such scaffolds display physical properties, such as viscosity, that

could be modulated by the concentration of chitosan (1-4%) (Sah *et al.*, 2019). The addition of 0.56M of Gp salt renders this hydrogel thermosensitive and its gelation at 37°C irreversible (Ganji *et al.*, 2007). Such properties are of high interest in the context of periodontal treatment to achieve efficient intra-pocket delivery. In the last decade, several chitosan-based hydrogels have been evaluated in the context of periodontitis treatment and periodontal regeneration in several animal models (Ismail, 2006; Lee *et al.*, 2016a; Lee *et al.*, 2016b; Özdogan *et al.*, 2018a; Özdogan *et al.*, 2018b). Indeed, such chitosan-based hydrogels were designed to allow release of active drugs including simvastatin (Ismail, 2006), lovastatin (Lee *et al.*, 2016a) and atorvastatin (Özdogan *et al.*, 2018b). Interestingly, Özdogan *et al.* evaluated chitosan-based hydrogel loaded with 2% atorvastatin in a ligature-induced periodontitis in rat (Özdogan *et al.*, 2018). They demonstrated that the daily application of such formulation improved significantly alveolar bone healing while no significant increase was observed in 2% atorvastatin in polyethylene glycol. Nevertheless, the anti-inflammatory effect associated with atorvastatin was enhanced by chitosan owing to its intrinsic anti-inflammatory and pro-healing properties (Saini *et al.*, 2020).

In order to increase aqueous solubility and to improve the bioavailability of atorvastatin and lovastatin, two lipophilic statins, a nanoemulsions-based drug delivery system has been successfully synthesized using vitamin E acetate associated with TPGS to encapsulate statins in nanodroplets. Vitamin E based nanoemulsions are biocompatible (Teixeira *et al.*, 2017) and their small size, below 200 nm, ensures good cellular uptake, greater stability, enhanced solubility, thereby, improving their biological activity (Salvia-Trujillo *et al.*, 2017).

Rodents have periodontal, anatomical, bacterial and pathogenic characteristics similar to humans (Saadi-Thiers *et al.*, 2013). However, the tiny size of the murine oral cavity presents a technical challenge in the placement of ligatures infected with periodontopathogenic bacteria necessary for the induction of periodontitis. To determine the

efficacy of atorvastatin TPGS nanoemulsions and lovastatin TPGS nanoemulsions, we selected a simplified model of induced bone defect. The calvarial defect model is frequently used in the evaluation of bone healing *in vivo*. Bone defects are easy to access, simple and quick to perform and sutures are inaccessible to the animal. In addition, the compressive force exerted on murine calvaria is similar to that in the intraoral wounds (Choi *et al.*, 2010). Mice, in which we produced calvarial defects of 2 mm, were thus treated with a deposit of 50 μ L of ChiG containing 0.1 mg of atorvastatin or lovastatin encapsulated or not in TPGS nanoemulsions in order to study the host reaction, *in vivo* stability and the capacity of atorvastatin and lovastatin for early bone regeneration. Interestingly, the histological analysis showed a greater bone neoformation in mice treated with atorvastatin TPGS nanoemulsions ChiG or lovastatin TPGS nanoemulsions ChiG in comparison with those treated by oral administration of the drugs. These results corroborate the previous studies where local application of 0.1 mg of statin constituted an appropriate dose for local application in animal model (Seyhan *et al.*, 2016; Türer *et al.*, 2016).

In this study, we selected atorvastatin and lovastatin due to their promising biological properties. They have been demonstrated to efficiently promote osteogenesis and to inhibit osteoclastic activity (Balli *et al.*, 2014; de Araújo Júnior *et al.*, 2013; Ho *et al.*, 2011; Lee *et al.*, 2016b; Mundy *et al.*, 1999). The results of our *in vitro* experiments show a gradual release of statins from ChiG allowing bioavailability of statins at the most opportune time of wound healing, *i.e* during the inflammatory phase (Morand *et al.*, 2017). This release within the initial days of healing causes a reduction in the inflammatory stimuli leading to the switch from inflammatory macrophages to wound healing macrophages at the inflammatory site (Fujishiro *et al.*, 2008) that orchestrate the transition of the inflammatory phase to the proliferative phase of healing (Diegelmann and Evans, 2004). In our study, atorvastatin TPGS nanoemulsions and lovastatin TPGS nanoemulsions significantly reduced *P.gingivalis*

induced inflammation via inhibiting TNF- α and IL-1 β expression and counteract *P.gingivalis* pro-resorptive effect through the reduction of RANKL expression as described in previous studies (de Araújo Júnior *et al.*, 2013; Fentoğlu *et al.*, 2012). Moreover, atorvastatin TPGS nanoemulsions and lovastatin TPGS nanoemulsions increased BSP2 expression in OB as observed for lovastatin in other cell types such as periodontal ligament cells (Kim *et al.*, 2011) confirming their pro-healing effect observed in bone.

In this study, the positive effects of atorvastatin TPGS nanoemulsions ChiG and lovastatin TPGS nanoemulsions ChiG were demonstrated *in vitro* on EC, FB and OB and *in vivo* in a calvarial defect model. This model is widely used in the context of bone regeneration (Eap *et al.*, 2015; Keller *et al.*, 2017), and, as described for the rat mandibular critical size model, is interesting to assess the efficacy of materials to augment bone formation (Graves *et al.*, 2012). However, as we aim to use this gel in the context of periodontal treatment, further experiments in experimental periodontitis model, such as ligature-induced periodontitis, should be conducted. Such model of periodontitis will allow to determine the effect of atorvastatin TPGS nanoemulsions ChiG and lovastatin TPGS nanoemulsions ChiG in an inflammatory and infectious environment.

5. Conclusion

The local delivery of atorvastatin TPGS nanoemulsions and lovastatin TPGS nanoemulsions may be of interest for the treatment of periodontitis lesion due to their interesting biological pro-regenerative properties. The use of such thermosensitive ChiG will allow clinicians to deliver active concentration of drugs at lesion site reducing the risk of side effects that may occur with systemic delivery. However, there is a need to confirm the observed results in the complex context of periodontitis.

Conflicts of interest

The authors declare that they have no competing financial interests or personal relationships that could have appeared to influence the work reported in this paper. This research did not receive any specific grant from funding agencies in the public, commercial, or not-for-profit sectors.

References

- Akncbay, H., Sene,l S., Ay, Z.Y., 2007. Application of chitosan gel in the treatment of chronic periodontitis. *J. Biomed. Mater. Res. Part B Appl. Biomater.* 80 : 290–296. <https://doi.org/10.1002/jbm.b.30596>
- Akram, Z., Abduljabbar, T., Kellesarian, S.V., Abu Hassan, M.I., Javed, F., Vohra, F., 2017. Efficacy of bisphosphonate as an adjunct to nonsurgical periodontal therapy in the management of periodontal disease: a systematic review. *Br J Clin Pharmacol.* 83 : 444–454. <https://doi.org/10.1111/bcp.13147>
- Aguilar, A., Zein, N., Harmouch, E., Hafdi, B., Bornert, F., Offner, D., Clauss, F., Fioretti, F., Huck, O., Benkirane-Jessel, N., Hua, G., 2019. Application of Chitosan in Bone and Dental Engineering. *Molecules.* 24. <https://doi.org/10.3390/molecules24163009>
- Aminu, N., Chan, S.-Y., Yam, M.-F., Toh, S.-M., 2019. A dual-action chitosan-based nanogel system of triclosan and flurbiprofen for localised treatment of periodontitis. *Int J Pharm.* 570 : 118659. <https://doi.org/10.1016/j.ijpharm.2019.118659>
- Anton, N., Benoit, J.-P., Saulnier, P., 2008. Design and production of nanoparticles formulated from nano-emulsion templates-a review. *J Control Release.* 128 : 185–199. <https://doi.org/10.1016/j.jconrel.2008.02.007>
- Anton, N. and Vandamme, T.F., 2009. The universality of low-energy nano-emulsification. *Int J Pharm.* 377 : 142–147. <https://doi.org/10.1016/j.ijpharm.2009.05.014>

Anton, N., Hallouard, F., Attia, M.F., Vandamme, T.F., 2016. Nano-emulsions for Drug Delivery and Biomedical Imaging, in: A. Prokop, V. Weissig (Eds.), *Intracellular Delivery III: Market Entry Barriers of Nanomedicines*. Springer International Publishing, Cham, 2016: pp. 273–300. https://doi.org/10.1007/978-3-319-43525-1_11

Balli, U., Keles, G.C., Cetinkaya, B.O., Mercan, U., Ayas, B., Erdogan, D., 2014. Assessment of vascular endothelial growth factor and matrix metalloproteinase-9 in the periodontium of rats treated with atorvastatin. *J. Periodontol.* 85 : 178–187. <https://doi.org/10.1902/jop.2013.130018>

Batool, F., Morand, D.-N., Thomas, L., Bugueno, I.M., Aragon, J., Irusta, S., Keller, L., Benkirane-Jessel, N., Tenenbaum, H., Huck, O., 2018. Synthesis of a Novel Electrospun Polycaprolactone Scaffold Functionalized with Ibuprofen for Periodontal Regeneration: An *In Vitro* and *In Vivo* Study. *Materials* 11. <https://doi.org/10.3390/ma11040580>

Batool, F., Agossa, K., Lizambard, M., Petit, C., Bugueno, I.M., Delcourt-Debruyne, E., Benkirane-Jessel, N., Tenenbaum, H., Siepmann, J., Siepmann, F., Huck, O., 2019. In-situ forming implants loaded with chlorhexidine and ibuprofen for periodontal treatment: Proof of concept study in vivo. *Int J Pharm.* 569 : 118564. <https://doi.org/10.1016/j.ijpharm.2019.118564>

Bedi, O., Dhawan, V., Sharma, P.L., Kumar, P., 2016. Pleiotropic effects of statins: new therapeutic targets in drug design. *Naunyn Schmiedebergs Arch. Pharmacol.* 389 : 695–712. <https://doi.org/10.1007/s00210-016-1252-4>

Bertl, K., Parllaku, A., Pandis, N., Buhlin, K., Klinge, B., Stavropoulos, A., 2017. The effect of local and systemic statin use as an adjunct to non-surgical and surgical periodontal therapy-A systematic review and meta-analysis. *J Dent.* 67 : 18–28. <https://doi.org/10.1016/j.jdent.2017.08.011>

Choi, J.-Y., Jung, U.-W., Kim, C.-S., Eom, T.-K., Kang, E.-J., Cho, K.-S., Kim, C.-K., Choi, S.-H., 2010. The effects of newly formed synthetic peptide on bone regeneration in rat calvarial defects. *J Periodontal Implant Sci.* 40 : 11–18. <https://doi.org/10.5051/jpis.2010.40.1.11>

de Araújo Júnior, R.F., Souza, T.O., de Moura, L.M., Torres, K.P., de Souza, L.B., Alves, M. do S.C.F., Rocha, H.O., de Araújo, A.A., 2013. Atorvastatin decreases bone loss, inflammation and oxidative stress in experimental periodontitis. *PLoS ONE.* 8 : e75322. <https://doi.org/10.1371/journal.pone.0075322>

Diegelmann, R.F and Evans, M.C., 2004. Wound healing: an overview of acute, fibrotic and delayed healing. *Front. Biosci.* 9 : 283–289. <https://doi.org/10.2741/1184>.

Donos, N., Calciolari, E., Brusseleers, N., Goldoni, M., Bostanci, N., Belibasakis, G.N., 2019. The adjunctive use of host modulators in non-surgical periodontal therapy. A systematic review of randomized, placebo-controlled clinical studies. *J. Clin. Periodontol.* doi: 10.1111/jcpe.13232. <https://doi.org/10.1111/jcpe.13232>

Eap, S., Keller, L., Schiavi, J., Huck, O., Jacomine, L., Fioretti, F., Gauthier, C., Sebastian, V., Schwinté, P., Benkirane-Jessel, N., 2015. A living thick nanofibrous

implant bifunctionalized with active growth factor and stem cells for bone regeneration.

Int J Nanomedicine. 4;10:1061-75. <https://doi.org/10.2147/IJN.S72670>

Emani, S., Gunjiganur, G.V., Mehta, D.S., 2014. Determination of the antibacterial activity of simvastatin against periodontal pathogens, *Porphyromonas gingivalis* and *Aggregatibacter actinomycetemcomitans*: An in vitro study. *Contemp Clin Dent.* 5 : 377–382. <https://doi.org/10.4103/0976-237X.137959>

Estanislau, I.M.G., Terceiro, I.R.C., Lisboa, M.R.P., Teles, P. de B., Carvalho, R. de S., Martins, R.S., Moreira, M.M.S.M., 2015. Pleiotropic effects of statins on the treatment of chronic periodontitis--a systematic review. *Br J Clin Pharmacol.* 79 : 877–885. <https://doi.org/10.1111/bcp.12564>

Fajardo, M.E., Rocha, M.L., Sánchez-Marin, F.J., Espinosa-Chávez, E.J., 2010. Effect of atorvastatin on chronic periodontitis: a randomized pilot study. *J. Clin. Periodontol.* 37 : 1016–1022. <https://doi.org/10.1111/j.1600-051X.2010.01619.x>

Fentoğlu, O., Kirzioğlu, F.Y., Ozdem, M., Koçak, H., Sütçü, R., Sert, T., 2012. Proinflammatory cytokine levels in hyperlipidemic patients with periodontitis after periodontal treatment. *Oral Dis.* 18 : 299–306. <https://doi.org/10.1111/j.1601-0825.2011.01880.x>

Fujishiro, N., Anan, H., Hamachi, T., Maeda, K., 2008. The role of macrophages in the periodontal regeneration using Emdogain gel. *J Periodont Res* 43 : 143-155. <https://doi.org/10.1111/j.1600-0765.2007.01004.x>

Ganji, F., Abdekhodaie, M.J., Ramazani S.A, A., 2007. Gelation time and degradation rate of chitosan-based injectable hydrogel, *J Sol-Gel Sci Technol.* 42 : 47–53. <https://doi.org/10.1007/s10971-006-9007-1>

Ganta, S., Deshpande, D., Korde, A., Amiji, M., 2010. A review of multifunctional nanoemulsion systems to overcome oral and CNS drug delivery barriers, *Mol. Membr. Biol.* 27 : 260–273. <https://doi.org/10.3109/09687688.2010.497971>

Gokhale, S.R. and Padhye, A.M., 2013. Future prospects of systemic host modulatory agents in periodontal therapy. *Br Dent J.* 214 : 467–471. <https://doi.org/10.1038/sj.bdj.2013.432>

Graves, D. T., Kang, J., Andriankaja, O., Wada, K., Rossa, C., 2012. Animal Models to Study Host-Bacteria Interactions Involved in Periodontitis. *Front Oral Biol.* 15:117-32. <https://doi.org/10.1159/000329675>

Graziani, F., Karapetsa, D., Alonso, B., Herrera, D., 2017. Nonsurgical and surgical treatment of periodontitis: how many options for one disease? *Perio 2000.* 75: 152-188. <https://doi.org/10.1111/prd.12201>

Grover, H.S., Kapoor, S., Singh, A., 2016. Effect of topical simvastatin (1.2 mg) on gingival crevicular fluid interleukin-6, interleukin-8 and interleukin-10 levels in chronic periodontitis – A clinicobiochemical study. *J Oral Biol Craniofac Res.* 6 : 85–92. <https://doi.org/10.1016/j.jobcr.2015.11.003>

Hajishengallis, G., 2015. Periodontitis: from microbial immune subversion to systemic inflammation. *Nat. Rev. Immunol.* 15: 30–44. <https://doi.org/10.1038/nri3785>

Ho, M.-H., Chiang, C.-P., Liu, Y.-F., Kuo, M.Y.-P., Lin, S.-K., Lai, J.-Y., Lee, B.-S., 2011. Highly efficient release of lovastatin from poly(lactic-co-glycolic acid) nanoparticles enhances bone repair in rats. *J. Orthop. Res.* 29 : 1504–1510. <https://doi.org/10.1002/jor.21421>

Ismail, F. A., 2006. Design and in Vitro Evaluation of Polymeric Formulae of Simvastatin for Local Bone Induction. *Drug Dev Ind Pharm.* 32(10):1199-206. <https://doi.org/10.1080/03639040600751886>

Joshi, D., Garg, T., Goyal, A.K., Rath, G., 2016. Advanced drug delivery approaches against periodontitis. *Drug Delivery.* 23 : 363–377. <https://doi.org/10.3109/10717544.2014.935531>

Keller L., Idoux-Gillet, Y., Wagner, Q., Eap, S., Brasse, D., Schwinté, P., Arruebo, M., Benkirane-Jessel, N., 2017. Nanoengineered implant as a new platform for regenerative nanomedicine using 3D well-organized human cell spheroids, *Int J Nanomedicine.* 12 : 447–457. <https://doi.org/10.2147/IJN.S116749>

Kim, I.S., Jeong, B.C., Kim, O.S., Kim, Y.J., Lee, S.E., Lee, K.N., Koh, J.T., Chung, H.J., 2011. Lactone form 3-hydroxy-3-methylglutaryl-coenzyme A reductase inhibitors (statins) stimulate the osteoblastic differentiation of mouse periodontal ligament cells via

the ERK pathway. *J. Periodont. Res.* 46 : 204–213. <https://doi.org/10.1111/j.1600-0765.2010.01329.x>

Kırzioğlu, F.Y., Tözüm Bulut, M., Doğan, B., Fentoğlu, Ö., Özmen, Ö., Çarsancaklı, S.A., Ergün, A.G., Özdem, M., Orhan, H., 2017. Anti-inflammatory effect of rosuvastatin decreases alveolar bone loss in experimental periodontitis. *J Oral Sci.* 59 : 247–255. <https://doi.org/10.2334/josnusd.16-0398>

Klymchenko, A.S., Roger, E., Anton, N., Anton, H., Shulov, I., Vermot, J., Mely, Y., Vandamme, T.F., 2012. Highly lipophilic fluorescent dyes in nano-emulsions: towards bright non-leaking nano-droplets. *RSC Adv.* 2 :11876–11886. <https://doi.org/10.1039/C2RA21544F>

Ko, H.H.T., Lareu, R.R., Dix, B.R., Hughes, J.D., 2017. Statins: antimicrobial resistance breakers or makers? *PeerJ.* 5. <https://doi.org/10.7717/peerj.3952>

Lee, B.-S., Lee, C.-C., Wang, Y.-P., Chen, H.-J., Lai, C.-H., Hsieh, W.-L., Chen, Y.-W., 2016a. Controlled-release of tetracycline and lovastatin by poly(d,l-lactide-co-glycolide acid)-chitosan nanoparticles enhances periodontal regeneration in dogs. *Int J Nanomedicine.* 11 : 285–297. <https://doi.org/10.2147/IJN.S94270>

Lee, B.-S., Lee, C.-C., Lin, H.-P., Shih, W.-A., Hsieh, W.-L., Lai, C.-H., Takeuchi, Y., Chen, Y.-W., 2016b. A functional chitosan membrane with grafted epigallocatechin-3-gallate and lovastatin enhances periodontal tissue regeneration in dogs. *Carbohydrate Polymers.* 151 : 790–802. <https://doi.org/10.1016/j.carbpol.2016.06.026>

Madi, M. and Kassem, A., 2018. Topical simvastatin gel as a novel therapeutic modality for palatal donor site wound healing following free gingival graft procedure. *Acta Odontol. Scand.* 76 : 212–219. <https://doi.org/10.1080/00016357.2017.1403648>

Martin-Cabezas, R., Davideau, J.-L., Tenenbaum, H., Huck O., 2016. Clinical efficacy of probiotics as an adjunctive therapy to non-surgical periodontal treatment of chronic periodontitis: a systematic review and meta-analysis. *J. Clin. Periodontol.* 43 : 520–530. <https://doi.org/10.1111/jcpe.12545>

Martínez-Ballesta, Mc., Gil-Izquierdo, Á., García-Viguera, C., Domínguez-Perles, R., 2018. Nanoparticles and Controlled Delivery for Bioactive Compounds: Outlining Challenges for New “Smart-Foods” for Health, *Foods*. 7. <https://doi.org/10.3390/foods7050072>

Mihaylova, B., Emberson, J., Blackwell, L., Keech, A., Simes, J., Barnes, E.H., Voysey, M., Gray, A., Collins, R., Baigent, C., 2012. The effects of lowering LDL cholesterol with statin therapy in people at low risk of vascular disease: meta-analysis of individual data from 27 randomised trials. *Lancet.* 380 : 581–590. [https://doi.org/10.1016/S0140-6736\(12\)60367-5](https://doi.org/10.1016/S0140-6736(12)60367-5)

Morand, D.N., Davideau, J.-L., Clauss, F., Jessel, N., Tenenbaum, H., Huck, O., 2017. Cytokines during periodontal wound healing: potential application for new therapeutic approach. *Oral Diseases.* 23 : 300–311. <https://doi.org/10.1111/odi.12469>

Mundy, G., Garrett, R., Harris, S., Chan, J., Chen, D., Rossini, G., Boyce, B., Zhao, M., Gutierrez, G., 1999. Stimulation of bone formation in vitro and in rodents by statins. *Science*. 286 ; 1946–1949. <https://doi.org/10.1126/science.286.5446.1946>

Muniz, F. W. M. G., Taminski, K., Cavagni, J., Celeste, R. K., Weidlich, P., Rösing, C. K., 2018. The effect of statins on periodontal treatment-a systematic review with meta-analyses and meta-regression. *Clin Oral Investig.* 22(2):671-687. <https://doi.org/10.1007/s00784-018-2354-9>

Nagy, K., Lán, g O., Láng, J., Perczel-Kovách, K., Gyulai-Gaál, S., Kádár, K., Köhidai, L., Varga, G., 2018. A novel hydrogel scaffold for periodontal ligament stem cells. *Interv Med Appl Sci.* 10 : 162–170. <https://doi.org/10.1556/1646.10.2018.21>

Özdoğan, A. I., Akca, G., Şenel, S. 2018a. Development and in vitro evaluation of chitosan based system for local delivery of atorvastatin for treatment of periodontitis. *Eur J Pharm Sci.* 124:208-216. doi: 10.1016/j.ejps.2018.08.037

Özdoğan, A.I., İlarslan, Y.D., Kösemehmetoğlu, K., Akca, G., Kutlu, H.B., Comerdiv, E., Iskit, A.B., Şenel, S.. 2018b. In vivo evaluation of chitosan based local delivery systems for atorvastatin in treatment of periodontitis. *Int J Pharm.* 550(1-2):470-476. <https://doi.org/10.1016/j.ijpharm.2018.08.058>

Petit, C., Batool, F., Bugueno, I.M., Schwinté, P., Benkirane-Jessel, N., Huck, O., 2019. Contribution of Statins towards Periodontal Treatment: A Review. *Mediators Inflamm.* 2019. <https://doi.org/10.1155/2019/6367402>

Pihlstrom, B.L., Michalowicz, B.S., Johnson, N.W., 2005. Periodontal diseases. *Lancet*. 366 1809–1820. [https://doi.org/10.1016/S0140-6736\(05\)67728-8](https://doi.org/10.1016/S0140-6736(05)67728-8)

Pina, S., Ribeiro, V.P., Marques, C.F., Maia, F.R., Silva, T.H., Reis, R.L., Oliveira, J.M., 2019. Scaffolding Strategies for Tissue Engineering and Regenerative Medicine Applications. *Materials* 12. <https://doi.org/10.3390/ma12111824>

Pradeep, A.R., Karvekar, S., Nagpal, K., Patnaik, K., Guruprasad, C.N., Kumaraswamy, K.M., 2015. Efficacy of locally delivered 1.2% rosuvastatin gel to non-surgical treatment of patients with chronic periodontitis: a randomized, placebo-controlled clinical trial, *J. Periodontol.* 86 : 738–745. <https://doi.org/10.1902/jop.2015.140631>

Pradeep, A.R., Kanoriya, D., Singhal, S., Garg, V., Manohar, B., Chatterjee, A., 2016. Comparative Evaluation of Subgingivally Delivered 1% Alendronate Versus 1.2% Atorvastatin Gel in Treatment of Chronic Periodontitis: A Randomized Placebo-Controlled Clinical Trial. *J Investig Clin Dent.* <https://doi.org/10.1111/jicd.12215>

Rao, N.S., Pradeep, A.R., Bajaj, P., Kumari, M., Naik, S.B., 2013. Simvastatin local drug delivery in smokers with chronic periodontitis: a randomized controlled clinical trial. *Aust Dent J.* 58 : 156–162. <https://doi.org/10.1111/adj.12042>

Saadi-Thiers, K., Huck, O., Simonis, P., Tilly, P., Fabre, J.-E., Tenenbaum, H., Davideau, J.-L., 2013. Periodontal and systemic responses in various mice models of experimental

periodontitis: respective roles of inflammation duration and *Porphyromonas gingivalis* infection. *J. Periodontol.* 84 : 396–406. <https://doi.org/10.1902/jop.2012.110540>

Sah, A.K., Dewangan, M., Suresh, P.K., 2019. Potential of chitosan-based carrier for periodontal drug delivery. *Colloids Surf B Biointerfaces.* 178 : 185–198. <https://doi.org/10.1016/j.colsurfb.2019.02.044>

Saini, S., Dhiman, A., Nanda. S., 2020. Immunomodulatory Properties of Chitosan: Impact on Wound Healing and Tissue Repair. *Endocr Metab Immune Disord Drug Targets.* <https://doi.org/10.2174/1871530320666200503054605>

Salvia-Trujillo, L., Soliva-Fortuny, R., Rojas-Graü, M.A., McClements, D.J., Martín-Belloso, O., 2017. Edible Nanoemulsions as Carriers of Active Ingredients: A Review. *Annu Rev Food Sci Technol.* 8 : 439–466. <https://doi.org/10.1146/annurev-food-030216-025908>

Sousa, L.H., Linhares, E.V.M., Alexandre, J.T., Lisboa, M.R., Furlaneto, F., Freitas, R., Ribeiro, I., Val, D., Marques M., Chaves, H.V., Martins, C., Brito, G.A.C., Goes, P., 2016. Effects of Atorvastatin on Periodontitis of Rats Subjected to Glucocorticoid-Induced Osteoporosis, *J. Periodontol.* 87 : 1206–1216. <https://doi.org/10.1902/jop.2016.160075>

Seyhan, N., Keskin, S., Aktan, M., Avunduk, M.C., Sengelen, M., Savaci, N., 2016. Comparison of the Effect of Platelet-Rich Plasma and Simvastatin on Healing of Critical-

Size Calvarial Bone Defects. *J Craniofac Surg.* 27 : 1367–1370.

<https://doi.org/10.1097/SCS.0000000000002728>

Subramanian, S., Emami, H., Vucic, E., Singh, P., Vijayakumar, J., Fifer, K.M., Alon, A., Shankar, S.S., Farkouh, M., Rudd, J.H.F., Fayad, Z.A., Van Dyke, T.E., 2013. A. Tawakol, High-dose atorvastatin reduces periodontal inflammation: a novel pleiotropic effect of statins. *J. Am. Coll. Cardiol.* 62 : 2382–2391. <https://doi.org/10.1016/j.jacc.2013.08.1627>

Teixeira, M.C., Severino, P., Andreani, T., Boonme, P., Santini, A., Silva, A.M., Souto, E.B., 2017. d- α -tocopherol nanoemulsions: Size properties, rheological behavior, surface tension, osmolarity and cytotoxicity. *Saudi Pharm J.* 25 : 231–235. <https://doi.org/10.1016/j.jsps.2016.06.004>

Thylin, M.R., McConnell, J.C., Schmid, M.J., Reckling, R.R., Ojha, J., Bhattacharyya, I., Marx, D.B., Reinhardt, R.A., 2002. Effects of simvastatin gels on murine calvarial bone. *J. Periodontol.* 73 : 1141–1148. <https://doi.org/10.1902/jop.2002.73.10.1141>

Türer, A., Türer, Ç.C., Balli, U., Durmuşlar, M.C., Önger, M.E., Çelik, H.H., 2016. Effect of Local Rosuvastatin Administration on Calvarial Bone Defects. *J Craniofac Surg.* 27 : 2036–2040. <https://doi.org/10.1097/SCS.0000000000002763>

Weitz-Schmidt, G., Welzenbach, K., Brinkmann, V., Kamata, T., Kallen, J., Bruns, C., Cottens, S., Takada, Y., Hommel, U., 2001. Statins selectively inhibit leukocyte function

antigen-1 by binding to a novel regulatory integrin site. *Nat. Med.* 7 : 687–692.
<https://doi.org/10.1038/89058>

Yang, C., Wu, T., Qi, Y., Zhang, Z., 2018. Recent Advances in the Application of Vitamin E TPGS for Drug Delivery. *Theranostics.* 8 : 464–485.
<https://doi.org/10.7150/thno.22711>. <https://doi.org/10.7150/thno.22711>

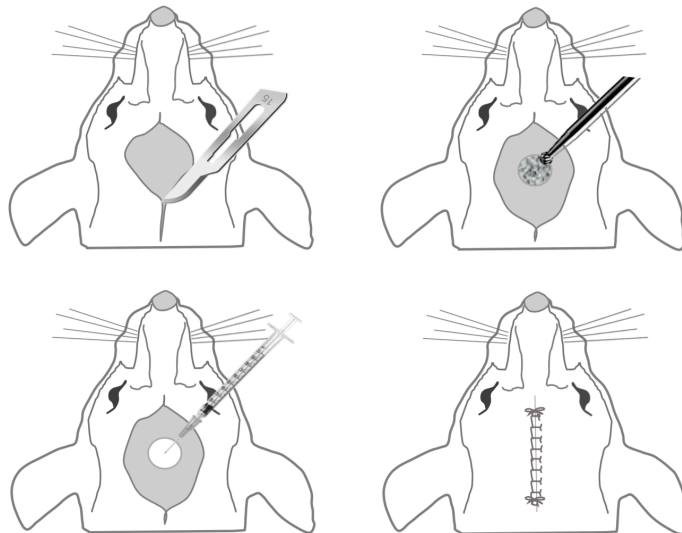
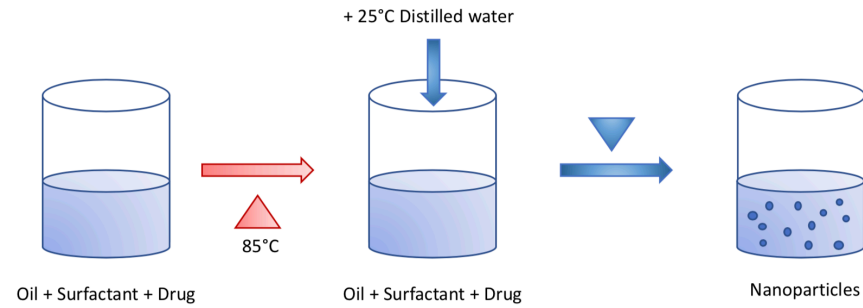
Zhang, Z., Tan, S., Feng, S.-S., 2012. Vitamin E TPGS as a molecular biomaterial for drug delivery. *Biomaterials.* 33 : 4889–4906. <https://doi.org/10.1016/j.biomaterials.2012.03.046>

Zhang, Y., Bradley, A.D., Wang, D., Reinhardt, R.A., 2014. Statins, bone metabolism and treatment of bone catabolic diseases. *Pharmacological Research.* 88 : 53–61.
<https://doi.org/10.1016/j.phrs.2013.12.009>

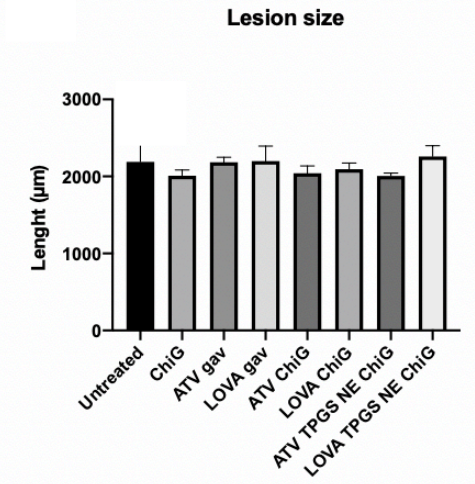
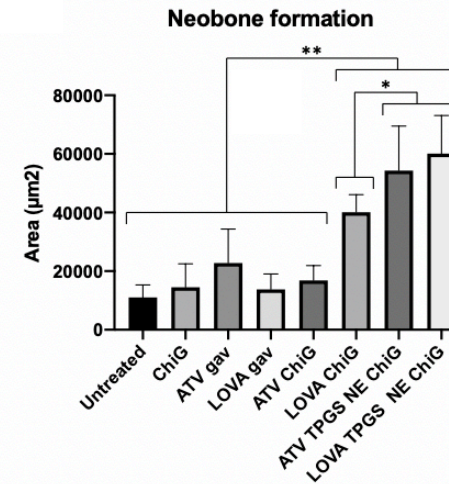
Synthesis and characterisation of statin loaded hydrogel

Biological properties of statin loaded hydrogel

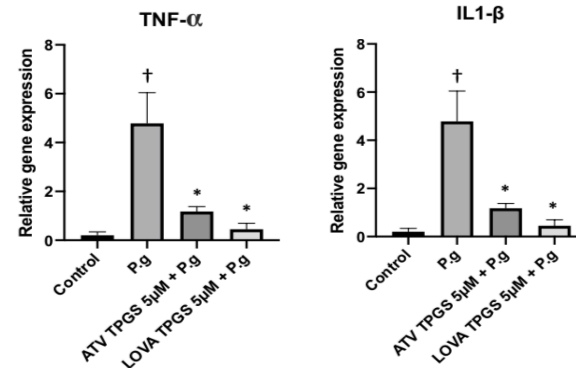
Formulation of statin loaded nanoemulsions



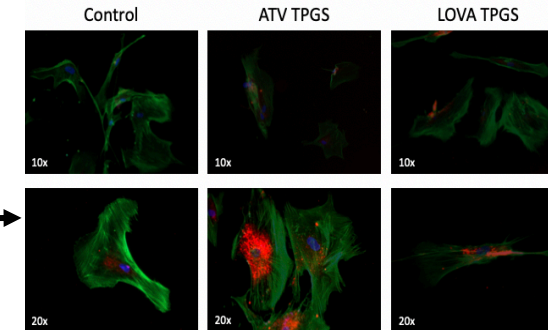
Improvement of bone regeneration



Anti-inflammatory properties



Pro-regenerative effect



Expression of Bone sialoprotein 2 in osteoblasts